



## Mixing within drops via surface shear viscosity

Shreyash Gulati<sup>a</sup>, Frank P. Riley<sup>a</sup>, Juan M. Lopez<sup>b</sup>, Amir H. Hirsaa<sup>a,\*</sup>

<sup>a</sup>Rensselaer Polytechnic Institute, Troy, NY, USA

<sup>b</sup>Arizona State University, Tempe, AZ, USA

### ARTICLE INFO

#### Article history:

Received 29 December 2017

Received in revised form 28 March 2018

Accepted 12 April 2018

#### Keywords:

Surface shear viscosity  
Drop shearing  
Drop mixing  
Containerless mixing  
Constrained drop  
Fluid dynamics

### ABSTRACT

A new strategy for mixing inside drops is introduced utilizing the action of surface shear viscosity. A drop is constrained by two sharp-edged contact rings that are differentially rotating. Differential rotation of the rings is conveyed by surface shear viscosity into the bulk fluid, thus enhancing the mixing when compared to the quiescent case. Primarily, mixing was considered in a configuration where one hemisphere is initially at a different concentration than the other. When inertia becomes important, the mixing time is reduced by an order of magnitude compared to the case where the two rings are stationary. Various driving speeds of one ring or counter rotation of two rings are considered for the hemispherical initial concentration. Mixing of a core-shell initial concentration was also considered. This approach to mixing in a drop is found to be an effective containerless mixer and may be utilized in chemical and biological applications where solid-wall interactions are deleterious.

© 2018 Elsevier Ltd. All rights reserved.

### 1. Introduction

Aqueous systems completely free of surface-active impurities are rarely found in nature or man-made systems, and their realization even in the laboratory is nearly impossible [1]. Any molecule that is amphiphilic, with both hydrophilic and hydrophobic parts, is thermodynamically favored to accumulate at the free surface, usually forming into a monomolecular layer. The presence of a monolayer generally reduces the surface tension,  $\sigma$ , in turn making the interface behave elastically and giving rise to the Marangoni stress. Monolayers can also give rise to two surface (excess) viscosities, namely the surface shear viscosity,  $\mu^s$ , and the surface dilatational viscosity,  $\kappa^s$  [2,3]. In many practical situations, the transport of mass, momentum, and energy are strongly affected by the viscoelastic nature of the monolayer [4].

Surface elasticity and its impact on the coupling between the bulk and interfacial flow via the Marangoni stress is well documented in the literature. Intrinsic surface viscosities are now receiving much attention, in part because of the interest in developing mechanistic models capable of predicting the flow in systems other than surface viscometers. Surface shear viscosity causes the interface to act like a membrane capable of propagating shear stress in the plane of the interface. Previously reported experiments [5,6] have unambiguously documented the dramatic effect that surface shear viscosity can have on bulk flow. On the

other hand, the action of surface dilatational viscosity is more complicated since it acts in unison with surface elasticity, and its characterization remains controversial [7–9].

A flow geometry consisting of a cylindrical dish where a circular knife edge touches the free surface is widely used to study surface shear viscosity. Recent numerical and centimeter-scale experimental studies of the flow in the knife-edge viscometer, including both steadily-driven and oscillatory-driven regimes, report a significant amount of flow in the bulk liquid, even for moderate values of surface shear viscosity [10–13]. The present study is inspired by those observations.

Here, we examine the flow in the bulk of a spherical drop, with the primary goal of exploiting its mixing capabilities. To form a centimeter scale spherical drop would require microgravity and such an effort is already being undertaken [14]. We explore mixing in millimeter-scale drops which can, in principle, be formed in the laboratory. Achieving mixing inside a drop is advantageous due to the reduced amount of reagents and waste generated, as well as the potential for faster mixing times [15,16]. Mixing within drops can also avoid contact between the drop liquid and solid walls, which may be deleterious in some applications due to sorption, chemical or electrostatic interactions. In systems involving microorganisms, complications due to wall adhesion are avoided by using a drop. Furthermore, in applications involving live cells or tissues, damage caused by large shear stresses found in bioreactors with blades or mixing bars is also avoided [17–20].

Several strategies for mixing within drops have been previously presented. One technique is to induce mixing in drops using a

\* Corresponding author.

E-mail address: [hirsaa@rpi.edu](mailto:hirsaa@rpi.edu) (A.H. Hirsaa).

serpentine microchannel [21]. A major challenge to drop mixing in microchannels is the low flow inertia. Other strategies for mixing inside drops impose direct excitation of the drop through various mechanisms, including electrowetting, acoustic, electric, magnetic or mechanical excitation [22–29]. Electrowetting, electric field and magnetic field excitation generally pose specific requirements on the electromagnetic properties of the fluid–solid system, restricting their applications. Another strategy for mixing within a drop is to use acoustic levitation and excitation. However, acoustic levitation leads to excessive heating of the fluid and relatively slow mixing due to the high frequencies involved [30]. Also, acoustic levitation requires sophisticated hardware to produce the high-frequency sound waves [31].

Fig. 1 shows a schematic of a ring-sheared drop, where the drop is constrained by two sharp-edged contact rings, one on the northern hemisphere and the other on the southern hemisphere. As will be shown in this paper, differential rotation of the rings imparts interfacial shear which in turn drives flow in bulk of the drop. Thus, surface shear viscosity can be used to set the fluid inside a drop into azimuthal motion without the need for a moving solid wall with large contact area. Furthermore, at non-negligible ring speeds, fluid inertia produces secondary meridional flow which enhances the mixing. It has been shown in the knife-edge viscometer that the thickness of the knife-edge only has a minor effect [32]. Thus, even in the limit of a contact circle (zero knife-edge thickness), the bulk fluid motion in the drop, including secondary meridional flow, is essentially the same as the bulk flow produced by a finite thickness knife edge [10]. Thus, for all practical purposes, the ring-sheared drop can be considered as a containerless droplet mixer.

For the present study, we consider a drop constrained between two rings at polar angles  $\theta = \pi/4$  and  $3\pi/4$  from the north pole, as shown schematically in Fig. 1. Several different ways of driving the ring-sheared drop are considered, including steady and oscillatory rotation of one ring, and the steady counter rotation of both rings. The quiescent case, corresponding to both rings being stationary, is the control case in which mixing is solely due to diffusion. Aside from the north–south initial distribution depicted in Fig. 1, we also consider mixing in a core–shell configuration.

## 2. Governing equations

Consider a drop of radius  $R$ , constrained between two rings of inner radius  $A = R/\sqrt{2}$ , with the top ring rotating at an angular speed of  $\Omega_1$  and the bottom ring rotating at  $\Omega_2$ . First, a north–south configuration of initial concentrations is considered, where the drop concentration is  $c_1$  in the northern hemisphere and  $c_2$  in the southern hemisphere. Then, mixing in a drop with an initial core–shell configuration is considered, where initially a core of high concentration is surrounded by a shell of relatively lower

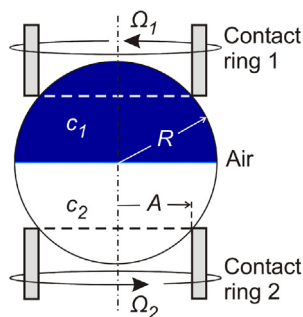


Fig. 1. Schematic of the ring-sheared drop with an initial north–south configuration. Blue represents a concentration of  $c_1$  and white represents a concentration of  $c_2$ . (For interpretation of the references to color in this figure legend, the reader is referred to the web version of this article.)

concentration. In the present study, these concentrations represent a passive scalar in the bulk liquid. This passive scalar–bulk liquid system forms a dilute solution such that the passive scalar does not change the viscosity of the solution,  $\nu$ . The binary diffusivity of the passive scalar in the solution is  $D$ . The ratio of these is the Schmidt number,  $Sc = \nu/D$ .

The flow in the drop is governed by the Navier–Stokes equations. Using  $R$  as the length scale and the viscous time  $R^2/\nu$  as the time scale, the non-dimensional Navier–Stokes equations are

$$\partial \mathbf{u} / \partial t + (\mathbf{u} \cdot \nabla) \mathbf{u} = -\nabla p + \nabla^2 \mathbf{u}, \quad \nabla \cdot \mathbf{u} = 0. \quad (1)$$

Using non-dimensional spherical coordinates  $(r, \theta, \phi)$ , where  $r$  is the radius,  $\theta$  is the polar angle and  $\phi$  is the azimuthal angle, the non-dimensional velocity is  $\mathbf{u} = (u, v, w)$  and  $p$  is the non-dimensional pressure.

Passive scalar transport in the drop is governed by an advection–diffusion equation, also non-dimensionalized with length scale  $R$  and time scale  $R^2/\nu$ , and  $c_1$  for the concentration. The non-dimensional advection–diffusion equation is

$$\partial c / \partial t + \mathbf{u} \cdot \nabla c = Sc^{-1} \nabla^2 c, \quad (2)$$

where  $c$  is the non-dimensional concentration. No-flux boundary condition for the concentration was applied at the free surface,  $r = 1$ .

For most of this study, the north–south configuration is considered, with the initial concentration set to  $c = 1$  in the upper half of the drop and  $c = 0$  in the lower half of the drop. This mimics the orientation of two coalesced drops of equal volume. Such a configuration has been produced experimentally (e.g. see Fig. 12 in Nowak et al. [33]). A core–shell initial configuration with  $c = 1$  in the core and  $c = 0$  in the shell is also considered.

The rings are non-wetting with sharp square corners so that they make circular contact lines on the surface of the drop ( $r = 1$ ) at polar angles  $\theta = \pi/4$  and  $3\pi/4$ . At these contact lines, there is no-slip and so the velocities are

$$(u, v, w)|_{\text{contact rings}} = (0, 0, Re_{1,2} A_r), \quad (3)$$

where  $Re_{1,2} = \Omega_{1,2} R^2 / \nu$  are the Reynolds numbers (ratios of viscous time to rotation time for each ring), with  $Re_1$  for the top ring and  $Re_2$  for the bottom ring, and  $A_r = A/R$  is the ratio of ring radius to drop radius (taken to be  $1/\sqrt{2}$ ).  $Re_1$  and  $Re_2$  are varied depending upon the configuration. We present results for three configurations: (i) the steady rotation of one ring with  $Re_1 = \text{constant}$  and  $Re_2 = 0$ , (ii) the oscillatory rotation of one ring with  $Re_1 = Re \sin \omega t$  and  $Re_2 = 0$ , and (iii) the steady counter rotation of the two rings with  $Re_1 = -Re_2 = \text{constant}$ .

The air–liquid interface is taken as non-deforming in this study. Thus, the surface stress balance in the radial (surface-normal) direction reduces to

$$u|_{r=1} = u^s = 0. \quad (4)$$

The tangential velocity boundary conditions on the interface are given by the stress balance between the bulk and interfacial flows through the Boussinesq–Scriven surface model [2,3,34]. This surface model is applicable to Newtonian interfaces and is based on a balance between the viscous stresses in the bulk and the various stresses on the interface, including stresses due to surface tension gradients and surface dilatational and shear viscosities. In this model, the surface stress tensor is given by:

$$\mathbf{T}^s = [\sigma + (\kappa^s - \mu^s) \nabla_s \cdot \mathbf{u}^s] \mathbf{I}_s + 2\mu^s \mathbf{D}^s, \quad (5)$$

where  $\nabla_s$  is the surface gradient operator,  $\mathbf{u}^s$  is the surface velocity vector,  $\mathbf{I}_s$  is the surface projection tensor and  $\mathbf{D}^s$  is the surface deformation tensor, such that

Download English Version:

<https://daneshyari.com/en/article/7054075>

Download Persian Version:

<https://daneshyari.com/article/7054075>

[Daneshyari.com](https://daneshyari.com)